Angewandte Chemie
International Edition

DOI: 10.1002/anie.201004015

Porphyrinoids

π Conjugation Transmitted across a d-Electron Metallocene in Ferrocenothiaporphyrin Macrocycles**

Irena Simkowa, Lechosław Latos-Grażyński, and Marcin Stępień*

The investigation of ferrocenophanes has been effectively stimulated by the search for useful starting building blocks for the preparation of new organometallic complexes and functional materials, efficient catalyst components, and redox-active modifiers of biomolecules.[1] The ability of ferrocenophanes to produce functional metallopolymers by ring-opening polymerization (ROP) provides a continuous momentum to the field.[2] The electronic properties of metallocene units embedded in *ansa* structures are of fundamental importance in determining their overall molecular properties (Scheme 1). However, in the majority of systems explored to date, the electronic communication between externally bridged cyclopentadienyl (Cp) rings was rather limited, as shown by structural and spectroscopic data.[3–5]

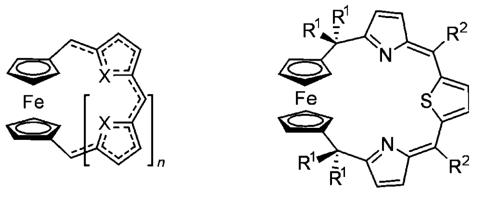

1 **2**, **2a**

Scheme 1. Incorporation of ferrocene into a porphyrinoid macrocycle. (**1:** X = N, NH, O, S; **2**: R^1 = Me, R^2 = tolyl (Tol), **2a**: R^1 = R^2 = H).

Another approach to probing the effectiveness of electronic conjugation across a sandwich complex is the incorporation of a metallocene subunit into an otherwise fully π-conjugated macrocycle. However, none of conjugated ferrocenophanes reported to date revealed features characteristic of macrocyclic aromaticity.[3–5] More recently, we have considered heterocyclic macrocycles of the general structure **1**, combining the structural features of *ansa*-metallocenes and porphyrinoids.[6] To date, a number of bridged pyrrolic *ansa*-ferrocene,[7] ferrocene–calixpyrrole,[8] and ferrocene–calixphyrin[6,9] hybrids have been reported (e.g., **2**),[6] which were based on a similar structural paradigm except that π conjugation in the oligopyrrin chain was interrupted by sp^3-hybridized meso bridges.

We have surmised that upon achieving complete conjugation in the oligopyrrin, the metallocene unit, occasionally described as a three-dimensional equivalent of π-electron aromatic units,[10] will contribute to metallomacrocyclic aromaticity in a similar fashion as various "two-dimensional" hetero- and carbocyclic rings commonly incorporated into porphyrinoid analogues.[11] Herein we report the synthesis and characterization of ferrocenothiaporphyrin **5** and dihydroferrocenothiaporphyrin **6**, which possess macrocyclic antiaromaticity and aromaticity, respectively. These two systems provide evidence for direct transmission of π-electron conjugation across a d-electron metallocene.

The title compound, ferrocenothiaporphyrin ([1-4,21-24,25,29η-25,29-dihydro-25,29-dicarba-27-thiapentapyrrin-25,29-diyl]iron(II)) **5**, was obtained in a [3+1] macrocyclization reaction that involved 1,1′-bis[phenyl(2-pyrrolyl)methyl]ferrocene **3** and 2,5-bis[hydroxy(*p*-tolyl)-methyl]thiophene **4**, which were condensed under Lindsey-type conditions (Scheme 2). After oxidation with 2,3-dichloro-5,6-dicyano-1,4-benzoquinone (DDQ) and column chromatography, the procedure afforded **5** as a dark brown compound in 9% yield.

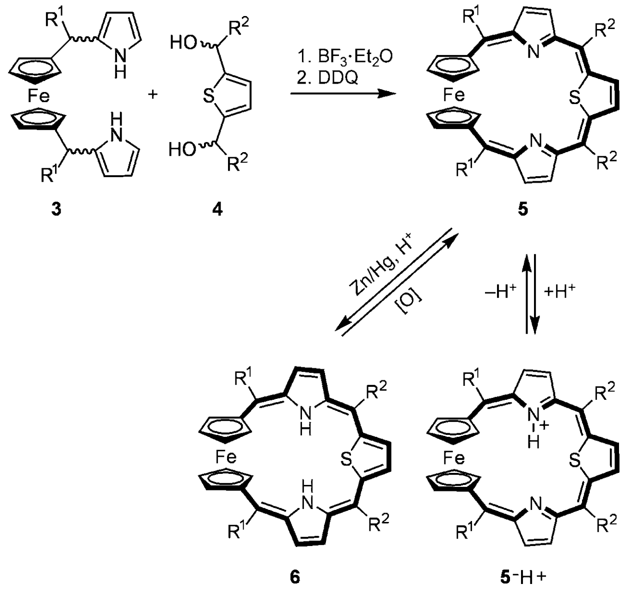

Scheme 2. Synthesis and reactivity of **5** and **6** (R^1 = Ph, R^2 = Tol). The partial π-electron pathway is shown in bold.

---

[*] I. Simkowa, Prof. L. Latos-Grażyński, Dr. M. Stępień
Department of Chemistry, University of Wrocław
14 F.Joliot-Curie St., 50-383 Wrocław (Poland)
Fax: (+48) 71-328-2348
E-mail: llg@wchuwr.pl
Homepage: http://llg.chem.uni.wroc.pl/

[**] Financial support from the Ministry of Science and Higher Education (Grant N N204 013536) is kindly acknowledged. DFT calculations were carried out at the Supercomputer Centers of Poznań and Wrocław.

Supporting information for this article is available on the WWW under http://dx.doi.org/10.1002/anie.201004015.

The molecular structure of **5**, obtained from an X-ray structural analysis, is shown in Figure 1.[12] The π system of **5** is uniformly torsionally distorted, with the dihedral angles of 25,29-dihydro-25,29-dicarba-27-thiapentapyrrin-25,29-diyl varying in the range −1.0–13.8°.

The bond lengths and angles in the ferrocene unit resemble those determined for the eclipsed conformer of plain ferrocene (average Fe–C 2.059 Å and C–C 1.431 Å).[13] The observed partial localization of double bonds in the 25,29-dihydro-25,29-dicarba-27-thiapentapyrrin-25,29-diyl is consistent with the valence bond structure of **5** (Scheme 2). The two cyclopentadienyl rings adopt an anticlinal eclipsed conformation (the C(4)-Ct-Ct′-C(21) torsional angle equals 144°, Ct, and Ct′ denote centroids of the respective Cp rings).

The electronic spectrum of **5** (Figure S16 in the Supporting Information) is significantly different from the spectrum of **2** both in appearance and intensity,[6] thus reflecting the influence of sp^2-hybridized meso bridges in **5** on the extent of π-conjugation. The absorption profile of **5** is dominated by a Soret-like band at 409 nm ($\log\varepsilon = 4.73$), which is accompanied by a broad and much less intense absorptions at 510 nm ($\log\varepsilon = 3.98$) and 735 nm ($\log\varepsilon = 3.62$).

Cyclic voltammograms recorded for **5** revealed one quasi-reversible oxidation process and one quasi-reversible and one irreversible reduction processes. The redox events are assigned to the 25,29-dicarba-27-thiapentapyrrin centered redox processes, that is, one-electron oxidation at 0.94 V and to two one-electron reductions at −1.36 V and −1.76 V (relative to ferrocene/ferrocenium (Fc/Fc$^+$)), respectively.

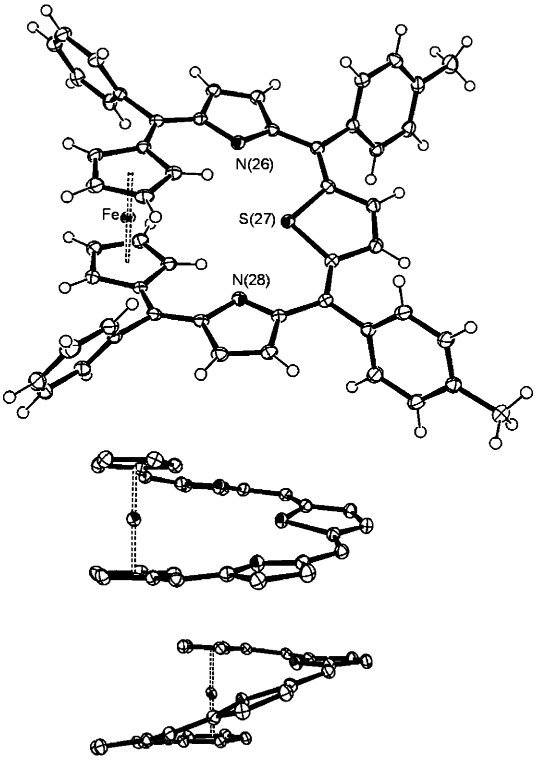

Figure 1. Crystal structure of **5** (top: perspective view, bottom: side views; aryl groups and hydrogen atoms omitted for clarity. Thermal ellipsoids represent 50% probability.

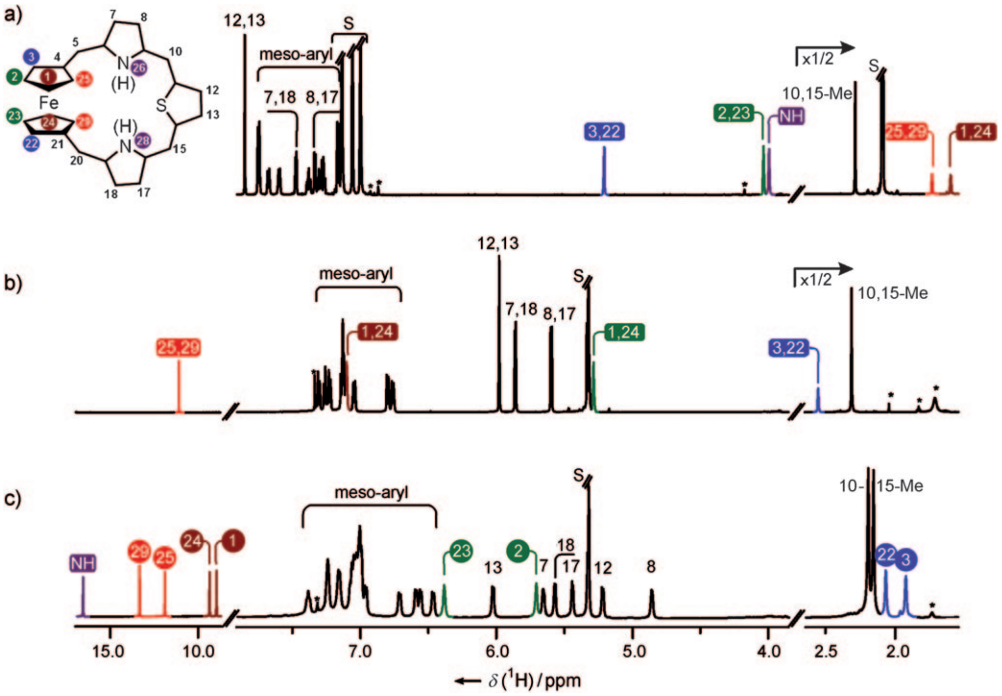

Figure 2. ^{1}H NMR spectra of a) aromatic **6** (250 K, [D$_8$]toluene), b) antiaromatic **5** (215 K, [D$_2$]dichloromethane), and c) **5**-H$^+$ (190 K, [D$_2$]dichloromethane). Resonance assignments follow the numbering given in (a).

The identity of **5** has been confirmed by high-resolution mass spectrometry and ^{1}H NMR spectroscopy. The assignment of resonances given for **5** in Figure 2 was made on the basis of relative intensities and detailed two-dimensional NMR analyses (involving COSY, NOESY, ^{1}H–^{13}C HMQC, and HMBC spectra) carried out between 190–300 K in [D$_2$]dichloromethane. The observed ^{1}H NMR spectrum of **5** is consistent with the C_2 symmetry of the helical molecular framework. The four ^{1}H resonances that correspond to the ferrocene-1,1′-diyl unit are found at 11.22 (H(25,29)), 7.10 (H(1,24)), 5.28 (H(2,23)), and 2.52 (H(3,22)) ppm, and serve as the fingerprint of an unprecedented electronic structure. To the best of our knowledge, such a large spread of chemical shifts (ca. 8.7 ppm) has not been detected for any ferrocene derivatives, including in particular *ansa*-ferrocenes that contain fully conjugated bridges.[4,5,14,15]

Titration of **5** with trifluoroacetic acid (190 K, [D$_2$]dichloromethane) affords a well-defined monocation **5**-H$^+$, which was observed by ^{1}H NMR spectroscopy. The protonation lowers the observed symmetry, thus rendering all positions inequivalent. The process can be readily reversed by addition of an amine base. Protonation takes place at the N(26) nitrogen atom, as confirmed by the rise of the corresponding N(26)H resonance at 11.64 ppm (Figure 2c), which reveals a scalar coupling to the H(7) and H(8) pyrrolic protons observable in the COSY map.

Reduction of **5** with zinc amalgam was performed in [D$_8$]toluene under strictly anaerobic conditions to yield the dihydroferrocenothiaporphyrin **6**. The macrocyclic diatropicity of this species is reflected by the chemical-shift pattern observed in the ^{1}H NMR spectrum (Figure 2a). At the intermediate stages of reduction, separate sets of resonances corresponding to **5** and **6** are clearly seen, indicating that the electron exchange between **5** and **6** is very slow on the ^{1}H NMR time scale. It is noteworthy that exposure of a solution of **6** in toluene to atmospheric dioxygen results in the quantitative recovery of **5** in a matter of hours. The UV/Vis spectrum of **6** (Figure S16 in the Supporting Information) shows a Soret-like absorption at 435 nm ($\log\varepsilon = 4.67$), and a broad band in the Q region (704 nm; $\log\varepsilon = 3.63$).

In the case of porphyrin analogues, ^{1}H NMR chemical shifts remain the convenient experimental measure of aromatic character,[11] and were proved to be equally applicable to porphyrinoid Hückel and Möbius systems.[16] Typically, protons that are located inside the macrocyclic ring and are strongly affected by ring currents serve as a sensitive aromaticity probe. Here, the most striking effect observed in the ^{1}H NMR spectra of **5**, **5**-H$^+$, and **6** is the unusual differentiation of chemical shifts within the ferrocene fragment (Figure 2). The spread of ferrocene shifts observed in **5** ($\delta = 11.30$–2.55 ppm) and **5**-H$^+$ ($\delta = 13.42$–1.55 ppm) is consistent with a macrocyclic paratropic ring current creating considerable magnetic anisotropy above and below the ring plane. This paratropic current also influences the shifts of pyrrole and thiophene β protons, which experience upfield relocations (relative to the non-aromatic reference system **2**) similar in magnitude to those observed in other paratropic Hückel[11,17,18] and Möbius[19] porphyrinoids (Figure 3).

Significantly, in the dihydro derivative **6**, the sign of the anisotropy is reversed, which is consistent with the presence of a diatropic current in the macrocycle. Indeed, the chemical shifts of peripheral protons on heterocyclic subunits are comparable with those reported for other porphyrinoids that display Hückel[20] or Möbius[11,18,21] aromaticity. This switching of the ring current sign upon formal two electron reduction/oxidation is a typical feature of π-electron aromatic species. In

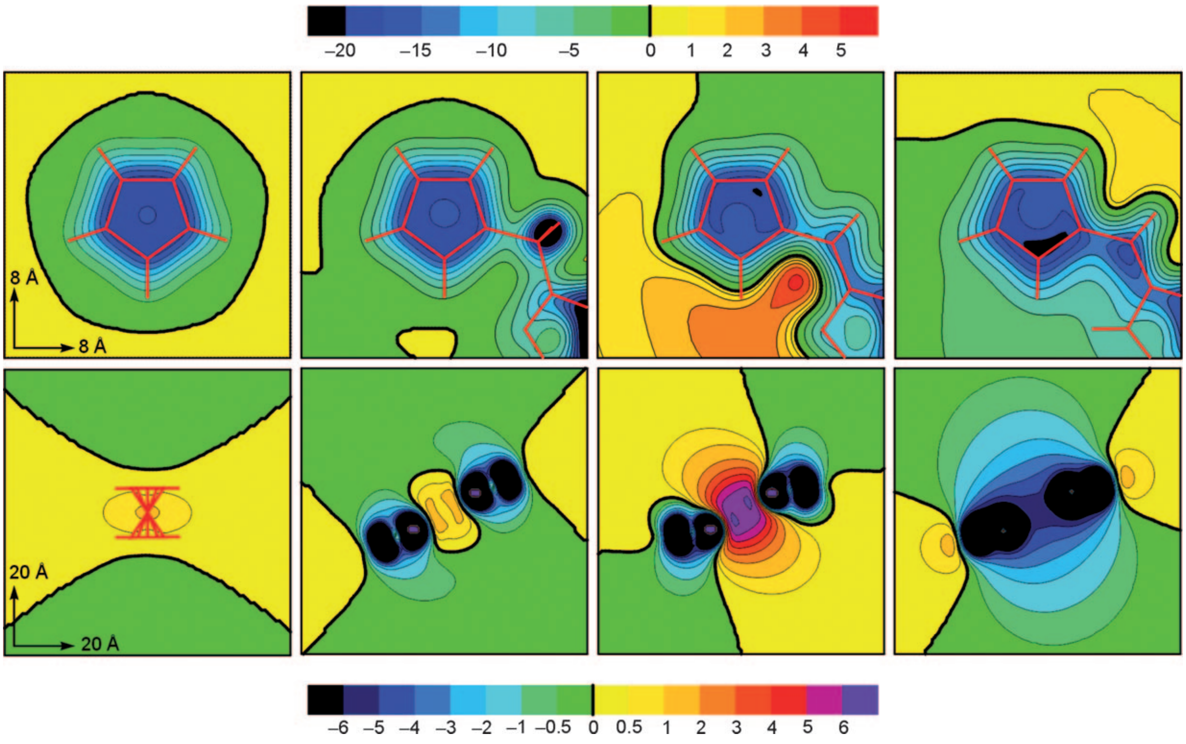

Figure 3. Through-space magnetic shielding contour maps calculated for ferrocene, **2a**, **5a**, and **6a**. Shielding signs are reversed to match the direction of the δ scale. Cross-sections shown in the top row are 1 Å above and parallel to the mean plane of the cyclopentadienyl ring. Cross-sections in the bottom have their normals aligned to the Fe–S vector and pass through the point located halfway between the two N atoms (see Figure S22 in the Supporting Information). For ferrocene, the plane was parallel to the fivefold axis and was chosen to lie 3.37 Å from the Fe atom, which is the average distance used for **5a** and **6a**. Skeletal projections of the molecules (red) are superimposed on some of the graphs. Color scales are different for the top and bottom rows.

the present case, however, the macrocyclic conjugation in **5** and **6** must necessarily involve the ferrocene iron atom, which principally participates in bonding with its d orbitals.

To gain further insight into the electronic structure of the new ferrocenoporphyrinoids, DFT calculations were performed for the meso-substituted species **2**, **5**, **5**-H$^+$, and **6** and some of their unsubstituted variants (**1a**, **5a**, and **6a**). Comparison of the geometries optimized for **5** and **6** at the B3LYP/LANL2DZ level of theory reveals that the effect of macrocyclic π-conjugation on the bond length is rather subtle. Specifically, the average $C_{ipso-\mathrm{Fc}}$-C_{meso} distances are 1.466 and 1.463 Å in **5** and **6**, respectively, and the bond lengths within the ferrocene subunits are only slightly perturbed relative to the equilibrium geometry of unsubstituted ferrocene optimized at the same level of theory (C–C 1.443 Å, Fe–C 2.121 Å). Comparison of the bond lengths in the tripyrrin section of **5** and **6** relative to the DFT-optimized geometries of their linear analogues that contain no ferrocene bridge (see the Supporting Information) shows that a weak bond-equalizing effect is indeed present in **6**, consistent with the observed aromaticity of this species. This effect however is not strong enough to provide a self-sufficient evidence for aromaticity of **6**.

As the essential experimental proofs for the aromaticity of **6** and antiaromaticity of **5** came from NMR spectroscopic data, we made an attempt to computationally reproduce the observed ring current effects. To this end, we evaluated GIAO (gauge-independent atomic orbital) chemical shieldings in appropriately chosen molecular cross sections by using an approach similar to that developed by Kleinpeter et al. (Figure 3).[22] We preferred this method to the more conventional uses of shielding calculations (either as nucleus-centered or nucleus-independent chemical shifts, see the Supporting Information for relevant data) because it enables easy visualization of the macrocyclic contribution to the overall ring current. To eliminate ring current contributions from meso substituents, DFT optimized geometries of unsubstituted structures **2a**, **5a**, and **6a** were used in the calculations. Comparison of the shielding cross sections passing through the center of the macrocycle (Figure 3, bottom row) reveals spectacular differences between the differently conjugated ferrocenoporphyrinoids. In the case of **2a**, small diatropic contributions from both pyrrole rings are seen, consistent with their residual local aromaticity. These two contributions are also seen in the cross-section obtained for **5a**, but in this case they are superimposed with a macrocyclic paratropic contribution, which gives rise to a characteristic deshielding zone above and below the center of the macrocycle. Conversely, in the aromatic macrocycle of **6a**, the diatropicity of the large ring adds to the ring currents of the pyrrole units, producing an extensive shielding zone above and below the macrocycle surface. The observed differences between **2a**, **5a**, and **6a** originate exclusively from macrocyclic contributions because the shielding from the ferrocene subunit is very weak at the distance of the macrocyclic cross-sections. The shielding zone in **5a** and deshielding zone in **6a** extend into the volume occupied by the ferrocene unit, as seen in the cross sections passing 1 Å above the Cp rings (Figure 3, top). The resulting unsymmetrical shielding environment is in agreement with the experimentally observed differentiation of chemical shifts observed in **5** and **6**.

In the simple yet very effective description of π conjugation in porphyrinoids known as the "annulene model", a monocyclic conjugation pathway (CP) is selected that 1) encompasses the macrocycle and 2) contains an alternating pattern of single and double bonds. A properly constructed CP is thus described by two Kekulé-like structures with a shifted double bond pattern. The electron count in the CP is then used to characterize the system as aromatic or antiaromatic, according to the Hückel rules[23] (for Hückel systems) or the Hückel–Heilbronner rules (for Möbius systems).[24] The major obstacle to applying the annulene model to **5** or **6** is that in each case the CP passes through the ferrocene subunit, which does not easily lend itself to the valence bond theoretical description.[25] On the other hand, the portion of the CP contained in the thiatripyrrin brace is easily identified in both **5** and **6** (and shown in bold in Scheme 2) and it contains 14 and 16 π electrons, respectively.

With the available experimental and computational data it is unclear whether one can select a single pathway passing through the ferrocene. Consequently, it is difficult to decide how many electrons of the metallocene actually participate in the CP and whether the pathway itself is of Hückel or Möbius type. Given the experimentally observed tropicities of **5** and **6**, the ferrocene subunit can be said to behave as a $(4m+2)$-electron reservoir without internal phase twist. These electronic properties result in a Hückel antiaromatic CP in **5** and a Hückel aromatic CP in **6**. However, if the ferrocene unit is assumed to introduce a phase shift to the orbital basis, it will act as a $(4m)$-electron reservoir, with **5** and **6** emerging as Möbius π-conjugated molecules. In fact, the two π-conjugation topologies can even coexist, as was suggested in earlier work on aromaticity of planar metallacycles.[26,27] Choosing between the Hückel and Möbius-type conjugation is not straightforward because of the properties of the d orbitals, which contribute to the macrocyclic conjugation in **5** and **6**.[27,28]

Porphyrins and porphyrinoids provide a uniquely versatile platform for exploration of macrocyclic π aromaticity. π-electron conjugation in porphyrin analogues depends on the topology of the molecular framework, conformation of the macrocycle, tautomerism, and metal coordination.[11] In appropriately designed macrocycles, it may result in a number of potentially useful features, such as multiple oxidation states, aromaticity switching through tautomeric equilibria, or the recently explored Möbius-type conjugation.[16,29] The present work reveals a hitherto unknown facet of porphyrinoid aromaticity, namely the possibility of including a d-electron subunit in a π-electron conjugation pathway. Further experimental work aiming to address the generalization of metallomacrocyclic aromaticity is currently in progress.

Received: July 1, 2010

Keywords: aromaticity · conjugation · macrocycles · metallocenes · porphyrinoids

---

[1] a) *Ferrocenes*: *Ligands*, *Materials and Biomolecules* (Ed.: P. Stepnicka), Wiley, Chichester, **2008**; b) D. R. van Staveren, N. Metzler-Nolte, *Chem. Rev.* **2004**, *104*, 5931–5985; c) G. R. Whittell, I. Manners, *Adv. Mater.* **2007**, *19*, 3439–3468.

[2] a) D. E. Herbert, J. B. Gilroy, W. Y. Chan, L. Chabanne, A. Staubitz, A. J. Lough, I. Manners, *J. Am. Chem. Soc.* **2009**, *131*, 14958–14968; b) S. Patra, G. R. Whittell, Y.-W. Wong, I. Manners, *Chem. Eur. J.* **2010**, *16*, 3240–3250.

[3] a) R. W. Heo, T. R. Lee, *J. Organomet. Chem.* **1999**, *578*, 31–42; b) J.-S. Park, T. R. Lee in *Modern Cyclophane Chemistry* (Eds.: R. Gleiter, H. Hopf), Wiley-VCH, Weinheim, **2005**, pp. 131–157.

[4] a) A. Kasahara, T. Izumi, *Chem. Lett.* **1978**, 21–24; b) A. Kasahara, T. Izumi, I. Shimizu, T. Oikawa, H. Umezawa, I. Hoshino, *Bull. Chem. Soc. Jpn.* **1983**, *56*, 1143–1148; c) I. Shimizu, Y. Kamei, T. Tezuka, T. Izumi, A. Kasahara, *Bull. Chem. Soc. Jpn.* **1983**, *56*, 192–198; d) I. Shimizu, H. Umezawa, T. Kanno, T. Izumi, A. Kasahara, *Bull. Chem. Soc. Jpn.* **1983**, *56*, 2023–2028; e) A. Kasahara, T. Izumi, H. Umezawa, *Chem. Lett.* **1980**, 1039–1042; f) A. Kasahara, T. Izumi, I. Shimizu, *Chem. Lett.* **1979**, 1119–1122.

[5] D. Tanner, O. Wennerstrom, *Acta Chem. Scand. Ser. B* **1980**, *34*, 529–535.

[6] M. Stępień, I. Simkowa, L. Latos-Grażyński, *Eur. J. Org. Chem.* **2008**, 2601–2611.

[7] a) M. Scherer, J. L. Sessler, A. Gebauer, V. M. Lynch, *Chem. Commun.* **1998**, 85–86; b) L. Sessler, R. S. Zimmerman, G. J. Kirkovits, A. Gebauer, M. Scherer, *J. Organomet. Chem.* **2001**, *637*, 343–348.

[8] S. Ramakrishnan, A. Srinivasan, *Org. Lett.* **2007**, *9*, 4769–4772.

[9] S. Ramakrishnan, K. S. Anju, A. P. Thomas, E. Suresh, A. Srinivasan, *Chem. Commun.* **2010**, *46*, 4746–4748.

[10] a) A. J. Locke, C. J. Richards, *Organometallics* **1999**, *18*, 3750–3759; b) J. Ma, M. Vollmann, H. Menzel, S. Pohle, H. Butenschon, *J. Inorg. Organomet. Polym.* **2008**, *18*, 41–50.

[11] a) M. Stępień, L. Latos-Grażyński *in Aromaticity in Heterocyclic Compounds*, *Vol. 19* (Eds.: T. M. Krygowski, M. K. Cyrański), Springer, Berlin, **2009**, pp. 83–154; b) M. Pawlicki, L. Latos-Grażyński in *Handbook of Porphyrin Science: With Applications to Chemistry*, *Physics*, *Materials Science Engineering*, *Biology and Medicine* (Eds.: K. M. Kadish, K. M. Smith, R. Guilard), World Scientific Publishing, Singapore **2010**, pp. 104–192.

[12] CCDC 782623 (**5**) contains the supplementary crystallographic data for this paper. These data can be obtained free of charge from The Cambridge Crystallographic Data Centre via www.ccdc.cam.ac.uk/data_request/cif.

[13] P. Seiler, J. D. Dunitz, *Acta Crystallogr. Sect. B* **1982**, *38*, 1741–1745.

[14] M. A. Buretea, T. D. Tilley, *Organometallics* **1997**, *16*, 1507–1510.

[15] A. Sudhakar, T. J. Katz, *J. Am. Chem. Soc.* **1986**, *108*, 179–181.

[16] M. Stępień, L. Latos-Grażyński, N. Sprutta, P. Chwalisz, L. Szterenberg, *Angew. Chem.* **2007**, *119*, 8015–8019; *Angew. Chem. Int. Ed.* **2007**, *46*, 7869–7874.

[17] M. Stępień, L. Latos-Grażyński, L. Szterenberg, *J. Org. Chem.* **2007**, *72*, 2259–2270.

[18] M. Stępień, B. Szyszko, L. Latos-Grażyński, *J. Am. Chem. Soc.* **2010**, *132*, 3140–3152.

[19] E. Pacholska-Dudziak, J. Skonieczny, M. Pawlicki, L. Szterenberg, Z. Ciunik, L. Latos-Grażyński, *J. Am. Chem. Soc.* **2008**, *130*, 6182–6195.

[20] L. Latos-Grażyński, J. Lisowski, M. M. Olmstead, A. L. Balch, *J. Am. Chem. Soc.* **1987**, *109*, 4428–4429.

[21] Z. S. Yoon, A. Osuka, D. Kim, *Nat. Chem.* **2009**, *1*, 113–122.

[22] E. Kleinpeter, S. Klod, A. Koch, *J. Mol. Struct. THEOCHEM* **2007**, *811*, 45–60.

[23] a) E. Hückel, *Z. Phys.* **1931**, *70*, 204–286; b) E. Hückel, *Z. Phys.* **1931**, *72*, 310–337.

[24] E. Heilbronner, *Tetrahedron Lett.* **1964**, *5*, 1923–1928.

[25] a) L. Pauling, *The Nature of the Chemical Bond*, Cornell University Press, Ithaca, NY, **1960**; b) F. Weinhold, C. R. Landis, *Valency and Bonding: A Natural Bond Orbital Donor–Acceptor Perspective*, Cambridge University Press, Cambridge, **2005**.

[26] a) Y. Z. Huang, S. Y. Yang, X. Y. Li, *J. Organomet. Chem.* **2004**, *689*, 1050–1056; b) I. Fernández, G. Frenking, *Chem. Eur. J.* **2007**, *13*, 5873–5884; c) L. J. Wright, *Dalton Trans.* **2006**, 1821–1827.

[27] M. Mauksch, S. B. Tsogogoeva, *Chem. Eur. J.* **2010**, *16*, 7843–7851.

[28] a) H. S. Rzepa, *Chem. Rev.* **2005**, *105*, 3697–3715; b) D. P. Craig, *J. Chem. Soc.* **1959**, 997–1001; c) D. P. Craig, N. L. Paddock, *Nature* **1958**, *181*, 1052–1053.

[29] Y. Tanaka, S. Saito, S. Mori, N. Aratani, H. Shinokubo, N. Shibata, Y. Higuchi, Z. S. Yoon, K. S. Kim, S. B. Noh, J. K. Park, D. Kim, A. Osuka, *Angew. Chem.* **2008**, *120*, 693–696; *Angew. Chem. Int. Ed.* **2008**, *47*, 681–684.